Appl Microbiol Biotechnol (2015) 99:10151–10161
DOI 10.1007/s00253-015-6898-1

Identification of the antiphagocytic trypacidin gene cluster in the human-pathogenic fungus *Aspergillus fumigatus*

Derek J. Mattern[1,2] · Hanno Schoeler[1,2] · Jakob Weber[1,2] · Silvia Novohradská[1,2] · Kaswara Kraibooj[2,3] · Hans-Martin Dahse[4] · Falk Hillmann[1] · Vito Valiante[5] · Marc Thilo Figge[2,3] · Axel A. Brakhage[1,2]

Received: 9 May 2015 / Revised: 26 July 2015 / Accepted: 29 July 2015 / Published online: 18 August 2015

Abstract The opportunistic human pathogen *Aspergillus fumigatus* produces numerous different natural products. The genetic basis for the biosynthesis of a number of known metabolites has remained unknown. The gene cluster encoding for the biosynthesis of the conidia-bound metabolite trypacidin is of particular interest because of its antiprotozoal activity and possible role in the infection process. Here, we show that the genes encoding the biosynthesis enzymes of trypacidin reside within an orphan gene cluster in *A. fumigatus*. Genome mining identified *tynC* as an uncharacterized polyketide synthase with high similarity to known enzymes, whose products are structurally related to trypacidin including endocrocin and fumicycline. Gene deletion of *tynC* resulted in the complete absence of trypacidin production, which was fully restored when the mutant strain was complemented with the wild-type gene. When confronted with macrophages, the *tynC* deletion mutant conidia were more frequently phagocytosed than those of the parental wild-type strain. This was also found for phagocytic amoebae of the species *Dictyostelium discoideum*, which showed increased phagocytosis of Δ*tynC* conidia. Both macrophages and amoebae were also sensitive to trypacidin. Therefore, our results suggest that the conidium-bound trypacidin could have a protective function against phagocytes both in the environment and during the infection process.

Keywords *Aspergillus fumigatus* · Genome mining · Trypacidin · Polyketide · Macrophage · *Dictyostelium discoideum*

Introduction

The biosynthetic potential of microorganisms producing different natural products (NPs) is vast and since the dawn of genome sequencing, this potential has been demonstrated by the surprising amounts of NP gene clusters unveiled (Brakhage 2013). To understand both the evolution of NPs and their ecological function, it is required to identify all the compounds and their corresponding gene clusters in a single fungal species. This will possibly give a hint on why distinct species encode for a certain type of gene clusters. Moreover, for a further understanding of the ecology of these compounds, the NPs of fungi growing in various habitats should be elucidated. This task is even more crucial in organisms that pose a risk to human health because understanding their complete metabolome will contribute to understanding the pathogenic cycle in patients. Here, we demonstrate this important task of assigning an already known and previously studied NP to its respective gene cluster in the opportunistic human pathogen *Aspergillus fumigatus*. This fungus is the most important

Electronic supplementary material The online version of this article (doi:10.1007/s00253-015-6898-1) contains supplementary material, which is available to authorized users.

✉ Axel A. Brakhage
axel.brakhage@hki-jena.de

[1] Department of Molecular and Applied Microbiology, Leibniz Institute for Natural Product Research and Infection Biology (HKI), Jena, Beutenbergstrasse 11a, 07745 Jena, Germany

[2] Friedrich Schiller University Jena, Jena, Germany

[3] Department of Applied Systems Biology, Leibniz Institute for Natural Product Research and Infection Biology (HKI), Jena, Germany

[4] Department of Infection Biology, Leibniz Institute for Infection Biology and Natural Product Research (HKI), Jena, Germany

[5] Leibniz Junior Research Group - Biobricks of Microbial Natural Product Syntheses, Jena, Germany

air-borne fungal pathogen to humans. The spores (conidia) of this fungus are ubiquitous and are constantly inhaled. *A. fumigatus* particularly poses a severe risk to immunocompromised individuals that may contract invasive aspergillosis leading to high mortality (Brakhage 2005; Heinekamp et al. 2015).

In particular, *A. fumigatus* produces a myriad of NPs and according to metabolomics studies on different *A. fumigatus* strains, it is estimated to produce over 230 NPs from 24 different biosynthesis families (Frisvad et al. 2009). What this shows is clearly the biosynthetic capacity of just one particular fungal species. Additionally, some of these compounds have been found to represent virulence determinants interacting with distinct responses of the immune system (Scharf et al. 2014a).

In the hunt for novel NPs in fungi, many different physiological and genetic strategies have been employed to activate silent NP gene clusters (Brakhage 2013). To help in pinpointing the exact correlation between the many different gene clusters, the known metabolites that have been previously discovered must also have their respective gene clusters identified. This will aid in finding the orphan gene clusters, which remain in an organism. To accomplish this, genome mining could be employed to compare similar known NP gene clusters to the unknowns, in order to identify similar compounds. In addition to *A. fumigatus*, this method has been employed in depth in the model organism *Aspergillus nidulans* (Bergmann et al. 2007; Yaegashi et al. 2014; Nielsen et al. 2011) and *Aspergillus terreus* known for its production of the cholesterol lowering compound lovastatin (Guo and Wang 2014); but interestingly, there still remains a very large amount of predicted gene clusters with unknown chemical products assigned.

In this study, our focus was on the metabolite trypacidin, which was originally identified in cultures of *A. fumigatus* roughly half a century ago (Nemec et al. 1963; Balan et al. 1963; Ebringer et al. 1963; Turner 1965). The metabolite was shown to be particularly active against the protozoa, e.g., *Toxoplasma gondii* and *Trypanosoma cruzi* (Balan et al. 1964). This conidium-born metabolite in *A. fumigatus* also showed to be a potent toxin to lung cells (Gauthier et al. 2012). Interestingly, fungi arm their conidia with ad hoc NPs. It was previously demonstrated that a compound structurally similar to trypacidin, endocrocin, was also accumulated in *A. fumigatus* conidia and showed immunosuppressive properties (Berthier et al. 2013). Thus, it can be deduced that arming their conidia can be a big advantage for fungi when encountering possible threats. Looking at it from the infection side, one of the first lines of defense in the mammalian immune system are macrophages, which ingest foreign materials such as pathogens (Ibrahim-Granet et al. 2003). When encountered with fungal conidia, it was shown that macrophages are able to phagocytose, acidify, and kill *A. fumigatus* conidia to a certain extent (Philippe et al. 2003; Thywißen et al. 2011; Mech et al. 2011). However, the natural product 1,8-dihydroxynaphthalene (DHN)-melanin, making the conidia gray-green, has the potential to inhibit acidification of phagolysosomes (Thywißen et al. 2011; Heinekamp et al. 2015). Furthermore, since the normal habitat of the fungus is usually soil (Brakhage and Langfelder 2002), it is not unlikely that it also encounters amoebae as environmental phagocytes. Previous studies have shown that in vitro, predatory organisms like *Acanthamoeba castellanii* or *Dictyostelium discoideum* can phagocytose *A. fumigatus* conidia efficiently (Van Waeyenberghe et al. 2013; Hillmann et al. 2015).

This study identifies the *A. fumigatus* trypacidin gene cluster. Additionally, *A. fumigatus* conidia lacking the ability to produce this compound were also shown to be more susceptible to being phagocytosed and killed by both human macrophages and *D. discoideum*, demonstrating the potential of this compound as a virulence determinant.

Materials and methods

Strains and cultivation

Strains used in this study were *A. fumigatus* Af293 (deposited, e.g., ATCC MYA-4609/CBS 101355/FGSC A1100) and *D. discoideum* strain AX2 (deposited at the Dicty Stock Center, Northwestern University, IL, USA). The authentic standard of trypacidin (Biomol, Hamburg, Germany) was also used as a reference in liquid chromatography-mass spectrometry (LC-MS) analysis and confrontation assays. Fungal cultures were prepared using *Aspergillus* minimal media (AMM) according to Then Bergh et al. (1996) and Maerker et al. (2005). *D. discoideum* was cultured in HL5 (Formedium, Norfolk, UK) with 1 % (*w*/*v*) of glucose. Fungal cultures for LC-MS analysis were grown in stationary liquid cultures at 37 °C for 72 h in AMM with a spore concentration of 1×10^7 spores/ml. Fresh conidia, not older than 2 weeks, were used and harvested from AMM agar plates with sterile water, strained with a 40 μm cell strainer (Bio Laboratories Pte Ltd., Singapore), counted with a CASY® TT Cell Counter (OLS Bio, Bremen, Germany), and stored at 4 °C. If necessary, hygromycin (InvivoGen, Toulouse, France) or pyrithiamine hydrobromide (Sigma-Aldrich, Taufkirchen, Germany) were added to the AMM agar plates.

Molecular techniques

Transformation of Af293 wild-type was conducted according to Unkles et al. (2014). Targeted gene replacement substituting the PKS gene (Afu4g14560/*tynC*) with hygromycin was used to create knock-outs. Primers used to generate the deletion cassette are listed in Table S1 in

the Supplementary Material, and the fusion construct was amplified according to Szewczyk et al. (2006). Knockouts were verified by Southern blot. For Southern blot analysis, 10 μg of chromosomal DNA of *A. fumigatus* was digested with *Bam*HI (New England Biolabs, Frankfurt, Germany). DNA fragments were separated on a 1 % (*w*/*v*) agarose gel and blotted onto a Roti®-Nylon plus membrane (Carl Roth, Karlsruhe, Germany). Labeling of the DNA probe was performed using 2× MyTaq Red Mix (Bioline, London, UK), DIG-11-dUTP (Jena Bioscience, Jena, Germany), and primers KO PKS Afu4g14560 P3 and P4 (Table S1 in the Supplementary Material). For detection of DNA–DNA hybrids, anti-digoxigenin-AP and the CDP-Star ready-to-use kit (Roche Applied Science, Mannheim, Germany) were used according to the manufacturer's instructions. Signals were detected using a Fusion FX-7 (Vilber Lourmat, Marne La Vallée, France). The complemented strain was completed accordingly, and pUC18 (Thermo Scientific, Schwerte, Germany) was linearized using the restriction enzyme *Sma*I (New England Biolabs, Frankfurt, Germany). Fragment #1 contains the 5′UTR and Afu4g14560/*tynC* PKS gene. It was amplified from genomic DNA of Af293 with the primers oJW0133/0128. Fragment #2 which contains the tef terminator and the ptrA cassette was amplified from pYES2 KanMX ptrA (Baldin et al. 2015) using primer pair oJW0134/0130. Fragment #3 harbors the 3′UTR of Afu4g14560/*tynC* and was amplified with the primers oJW0135/0136. All three fragments were produced with 20–30 bp overlaps to the neighboring fragments using mentioned primers (see also Table S1 in the supplementary materials) and 2× Phusion High-Fidelity PCR Master Mix (Life Technologies, Darmstadt, Germany). Assembly of the fragments as well as linearized pUC18 was conducted with Gibson cloning according to the manufacturer's guidelines; completed plasmid (Fig. S1 in Supplementary Material) was transformed into the ΔAfu4g14560/*tynC* as described above (New England Biolabs, Frankfurt, Germany; Gibson et al. 2009).

Genome mining for putative polyketide synthase gene

BLASTP searches were conducted on the *Aspergillus* Genome Database (AspGD) (Cerqueira et al. 2013), using the genomes of *A. nidulans* FGSC A4 and *A. fumigatus* Af293. The GENE IDs for the analyzed PKSs are as follows: monodictyphenone (AN0150/*mdpG*), asperthecin (AN6000/*aptA*), endocrocin (Afu4g00210/*encA*), fumicycline (Afu7g00160/*fccA*), and geodin (ATEG_08451/GedC). For the analysis of the PKS domains, the management and analysis for polyketide synthase type I (MAPSI) (Tae et al. 2009) and conserved domain analysis (CDD) (Marchler-Bauer et al. 2002) were used and compared. For alignment of the different PKS domains, Vector NTI advanced 9.1 (Invitrogen, Darmstadt, Germany) was used.

Extraction and chemical analysis

Stationary cultures were grown for 72 h at 37 °C, then homogenized using a Polytron® PT 1200 (Kinematica, Luzern, Switzerland) and extracted with 2× (*v*/*v*) ethyl acetate. The organic phase was dried with anhydrous sodium sulfate, filtered, and then concentrated with a rotary evaporator. The crude extract was dissolved in 1 ml of methanol filtered again with a 0.2 μm PTFE filter (Carl Roth, Karlsruhe, Germany). Samples were injected onto an LC-MS system consisting of an HPLC: UltiMate 3000 binary RSLC with photo diode array detector (Thermo Fisher Scientific, Dreieich, Germany) and the mass spectrometer (LTQ XL Linear Ion Trap from Thermo Fisher Scientific, Dreieich, Germany) with an electrospray ion source. HPLC method consisted of using an ACCUCORE RP-MS 2.6 μm 150 × 4.6 mm column (Thermo Fisher Scientific, Dreieich, Germany) with the following gradient: initial MeCN/0.1 % (*v*/*v*) HCOOH (H_2O) 0/100 and increasing to 80/20 in 15 min, then to 100/0 in 2 min, 2 min 100/0, and then back to 0/100 in 2 min with a flow rate 1 ml/min and injection volume of 10 μl. The high-resolution mass spectrometry data was measured on an Exactive Orbitrap high-performance Benchtop LC-MS with an electrospray ion source and an Accela HPLC system (Thermo Fisher Scientific, Bremen, Germany) equipped with a C18 column (Betasil C18 3 μm 150 × 2.1 mm).

Confrontation of macrophages with conidia

Murine alveolar MH-S macrophages (ATCC CRL-2019TM) were cultivated in RPMI 1640 medium supplemented with 10 % (*v*/*v*) FCS (Thermo Fisher Scientific, Dreieich, Germany), 1 % (*v*/*v*) sodium bicarbonate (Lonza, Cologne, Germany), and 0.05 mM beta-mercaptoethanol (Life Technologies, Darmstadt, Germany). The cells were seeded on glass cover slips in 24-well plates at a density of 3×10^5 cells per well and allowed to grow adherently overnight. The conidia were stained with fluorescein isothiocyanate (FITC; Sigma-Aldrich, Taufkirchen, Germany) for 30 min at 37 °C while shaking. After washing them three times with PBS, 0.01 % (*v*/*v*) Tween 20 (AppliChem, Darmstadt, Germany), they were added to the macrophages at a multiplicity of infection (MOI) of 7. Synchronization of the experiment was realized by centrifugation for 5 min at 100 g and 37 °C. To initiate the experiment, the co-incubation was shifted to a CO_2 incubator for 1 h at 37 °C. The cells were fixed for 45 min at room temperature by adding 16 % (*v*/*v*) paraformaldehyde (Electron

Microscopy Sciences, Munich, Germany) directly to the medium to a concentration of 1 % (*v*/*v*). After two washing steps, extracellular conidia were stained with PBS 0.1 mg/ml calcofluor white (CFW; Sigma-Aldrich, Taufkirchen, Germany) for 30 min at room temperature. The cells were washed again twice with PBS. Prior to antibody labeling, binding sites were blocked with PBS, 3 % (*w*/*v*) BSA Fraction V (AppliChem, Darmstadt, Germany) for 30 min. Next, macrophages were labeled with a monoclonal rat anti-CD9 antibody (1:200; Santa Cruz Biotechnology, Heidelberg, Germany) over night at 4 °C and an Alexa Fluor® 647 goat anti-rat IgG antibody (1:200; Life Technologies, Darmstadt, Germany) for 1.5 h at room temperature.

Microscopy images were taken on a Zeiss LSM 780 Live confocal laser scanning microscope with a 20× Zeiss plan-apochromat dry objective (0.8 NA; Zeiss, Jena, Germany). Each image consists of 1024 × 1024 pixels with a pixel size of 0.2 μm. For each strain, we analyzed two technical and two biological replicates. Fifteen images were taken per technical replicate, which made 60 images in total per strain.

Automated image analysis

Image analysis was performed by an algorithm developed within Definiens Developer XD framework (Definiens, Munich, Germany). Variations of this algorithm were previously implemented and rigorously validated to quantify host–pathogen interactions, including phagocytosis assays for *A. fumigatus* conidia (Mech et al. 2011). Each image consists of three layers, one for each fluorescent label: green layer contains all *A. fumigatus* conidia, blue layer contains all non-phagocytosed conidia, and red layer contains all macrophages.

The algorithm comprises three steps: (i) pre-processing, (ii) segmentation, and (iii) classification. In the pre-processing step, noise in the images was reduced by a Gauss filter (with a width of σ=5 px for the red layer and σ=1 px for the green layer). The segmentation step was performed in analogy to previous implementations (Mech et al. 2011, 2014; Kraibooj et al. 2014), where regions of interest (ROI) were recognized based on watershed segmentation and on the combination of ROI intensity and morphology (area, roundness, and length-to-width ratio). Finally, in the classification step, we distinguished between phagocytosed and non-phagocytosed conidia by comparing the blue layer with the green layer, and we distinguished whether non-phagocytosed conidia were adherent or non-adherent to macrophages by examining the blue layer for spatial proximity of conidia to macrophages in the red layer. A typical example of the algorithm for automated image analysis is presented in Fig. S2 in the Supplementary Material.

Upon automated image analysis, all conidia in the images (N_{all}: 4907 for Af293 and 5026 for ΔAfu4g1460/*tynC*) were classified as being either phagocytosed conidia (N_{phag}: 3843 for Af293 and 4369 for ΔAfu4g1460/*tynC*) or macrophage-adherent conidia (N_{adh}: 966 for Af293 and 547 for ΔAfu4g1460/*tynC*). The quantitative comparison for phagocytosis between strains was performed by computing the phagocytosis ratio $p_r=N_{phag}/(N_{phag}+N_{adh})$ and the statistical evaluation for significant differences was performed by the Wilcoxon rank-sum test.

Cytotoxicity of trypacidin with macrophages

Trypacidin was assayed against the murine alveolar macrophages MH-S (ATCC 2019) for its cytotoxic effect. The cells were cultivated in RPMI 1640 (Lonza, Verviers, Belgium) supplemented with 10 % (*v*/*v*) heat-inactivated fetal bovine serum (ATCC 30-2020), 1 % (*w*/*v*) ultraglutamine 1 (Lonza), 0.05 mM 2-mercaptoethanol (Life Technologies, Darmstadt, Germany), 1 % (*v*/*v*) sodium pyruvate solution (Lonza, Verviers, Belgium), and 550 μl/l (50 mg/ml) gentamicin sulfate (Lonza) at 37 °C in 5 % CO_2. For each of four replicates, approximately 10,000 cells were seeded with 0.1 ml RPMI 1640 medium into 96-well microplates (Thermo Fisher Scientific, Dreieich, Germany). The cells were incubated with different concentrations of the test compounds for 72 h at 37 °C in a humidified atmosphere and 5 % CO_2. For estimating the influence of trypacidin on viable cells, we used the CellTiter-Blue® assay (Promega, Mannheim, Germany). Thus, the absorbance measurement at 570 nm and using 600 nm as a reference wavelength can be used to monitor results. Values are compared to blank well containing CellTiter-Blue® reagent without cells. Under our experimental conditions, the signals from the CellTiter-Blue® reagent are proportional to the number of viable cells. A repeat determination has been conducted in all experiments; four replicates were assayed. The calculations of the 50 % cytotoxicity concentration, CC50 values were performed with the software MAGELLAN (Tecan, Crailsheim, Germany).

Amoebicidal effects of trypacidin

Cells of *D. discoideum* were initially grown as described earlier (Hillmann et al. 2015) and seeded into 48-well plates at a final concentration of 1×10^5 cells/ml. To determine potential amoebicidal effects, surface adherent amoeba were either exposed to viable conidia of *A. fumigatus* at an MOI of two or to pure trypacidin dissolved in DMSO. Cells were incubated at 22 °C for further 24 h and the number of amoeba cells was determined in a CASY® TT Cell Counter (OLS Bio, Bremen, Germany). The inhibitory concentration (IC_{50}) was calculated

by fitting a four-parameter dose response logistic function, obtained when the fraction of growth inhibition was plotted against the log values of the toxin concentration in Origin® software (OriginLab, Northampton, MA).

For fluorescent labeling, fungal conidia were resuspended in 0.1 M Na_2CO_3 and incubated with 0.1 mg/ml FITC (Sigma-Aldrich, Taufkirchen, Germany) at 37 °C for 30 min using a thermomixer. Unbound FITC was washed out by PBS containing 0.1 % (*w*/*v*) Tween 20. Stained conidia were used in confrontation with *D. discoideum*, grown overnight at 22 °C in HL5 medium with 1 % (*w*/*v*) of glucose. For fluorescence microscopy of phagocytosis, the medium was exchanged for 0.2xHL5 with 1 % (*w*/*v*) of glucose, and conidia were added at an MOI of 10. After 1 h of co-incubation, the medium was aspirated and replaced by PBS with 0.5 mg/ml CFW (Sigma-Aldrich, Taufkirchen, Germany) for 10 min. Finally, cells were fixed using PBS with 16 % (*v*/*v*) paraformaldehyde (Electron Microscopy Sciences, München, Germany) for 10 min and immediately visualized using a Zeiss LSM 5-Live microscope (Zeiss, Jena, Germany) and processed with ZEN imaging software (Zeiss, Jena, Germany). The number of ingested conidia per amoeba was determined by counting internalized conidia in a total number of 200 amoebae in 3 biological replicates.

Results

Genome mining and identification of the trypacidin biosynthesis gene cluster

As the genes involved in trypacidin biosynthesis were unknown, we first selected several, structurally related compounds for which the corresponding polyketide synthases (PKSs) have been assigned (Fig. 1a). These were namely the monodictyphenone (GENE ID: AN0150/*mdpG*; Chiang et al. 2010) and asperthecin (Gene ID: AN6000/*aptA*; Szewczyk et al. 2008) biosynthesis in *A. nidulans*, endocrocin (GENE ID: Afu4g00210/*encA*; Lim et al. 2012) and fumicycline (GENE ID: Afu7g00160/*fccA*; König et al. 2013; Chooi et al. 2013) biosynthesis in *A. fumigatus*, and geodin

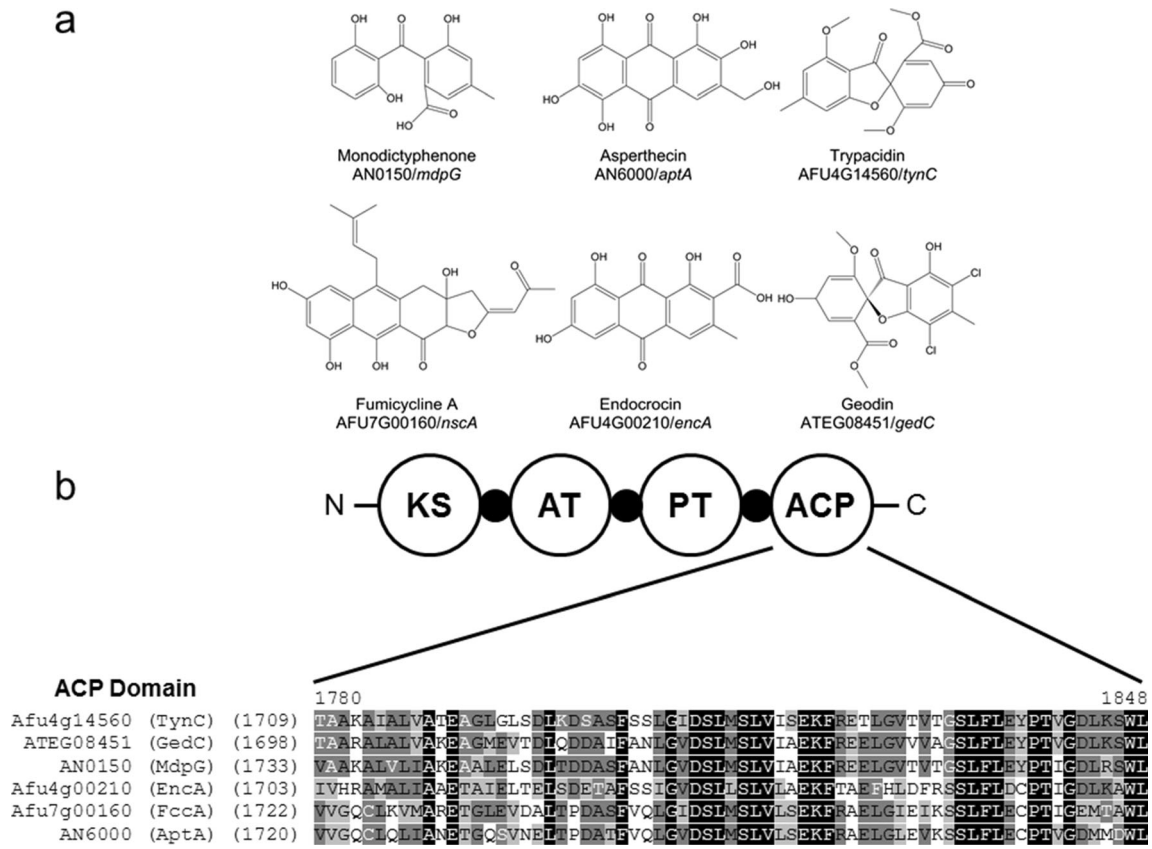

Fig. 1 Genome mining of the Afu4g14560/TynC PKS. **a** Structurally similar polyketide products: monodictyphenone and asperthecin from *A. nidulans* and fumicycline A, endocrocin, and trypacidin from *A. fumigatus* and geodin from *A. terreus* (Chiang et al. 2010; Szewczyk et al. 2008; Lim et al. 2012; König et al. 2013; Chooi et al. 2013; Nielsen et al. 2013). **b** Composition of the PKS domains conserved among the four PKSs analyzed: ketosynthase (KS), acyltransferase (AT), product template (PT), and acyl carrier protein (ACP). **C** Amino acid alignment of the ACP domains of the different PKSs

(GENE ID: ATEG_08451/GedC; Nielsen et al. 2013) from *A. terreus*. The similarity of these compounds stems from their compound class anthraquinones, from which they all are derived (Gauthier et al. 2012). A protein blast search against the genomes of *A. fumigatus* using the deduced amino acid sequences of these known PKS-encoding genes as templates identified Afu4g14560/*tynC* as a putative unknown PKS with highest amino acid similarity to the ATEG_08451/GedC geodin PKS. Furthermore, the Afu4g14560/*tynC* gene encoded for a non-reducing PKS with domains consisting of an acyl carrier protein (ACP), product template (PT), acyltransferase (AT), and a ketoacyl synthase (KS) domains (Fig. 1b). These domains were conserved among the six other PKSs mentioned above. The amino acid sequences between the different domains are also highly conserved (Fig. 1b and S3a–c in the Supplementary Material). Additionally, its genomic context reveals Afu4g14560/*tynC* as the only PKS-encoding gene within the putative biosynthesis cluster (Fig. 2a) that is localized near the subtelomeric region on the long arm of chromosome IV. The predicted cluster encodes a variety of tailoring enzymes that could potentially be involved in the biosynthesis. Moreover, a comparison of the putative trypacidin biosynthetic pathway with the previously studied geodin cluster was also used comparing the amino acid identity of all orthologous genes between the two clusters (Table 1). The similarity between the two pathways is astonishing with only one enzyme extra in the trypacidin pathway, Afu4g14510/TynH.

Furthermore, to test if Afu4g14560/*tynC* encoded the PKS for the biosynthesis of trypacidin, the entire gene was deleted (Fig. 2a), and its absence was verified by Southern blot (Fig. 2b). Two independent knock-out mutants were generated and both were shown not to produce trypacidin; only one strain was used for further analysis. We named the PKS for trypacidin TynC and thus the corresponding deletion strain Δ*tynC*. This strain was tested for NP analysis by LC-MS. In accordance with previous studies, trypacidin could only be detected in the wild-type strain of Af293 under sporulation conditions (Parker and Jenner 1968; Fischer et al. 1999; Gauthier et al. 2012). When analyzing stationary cultures of the two strains, trypacidin was only identified in the *A. fumigatus* Af293 wild-type, while no trypacidin was found in the deletion mutants when compared to an authentic standard (Fig. 2c–2e). This clearly suggested that the PKS encoded by *tynC* (accession number: Afu4G14560) was responsible for trypacidin biosynthesis. To better understand if this pathway is correct according to previous studies, high-

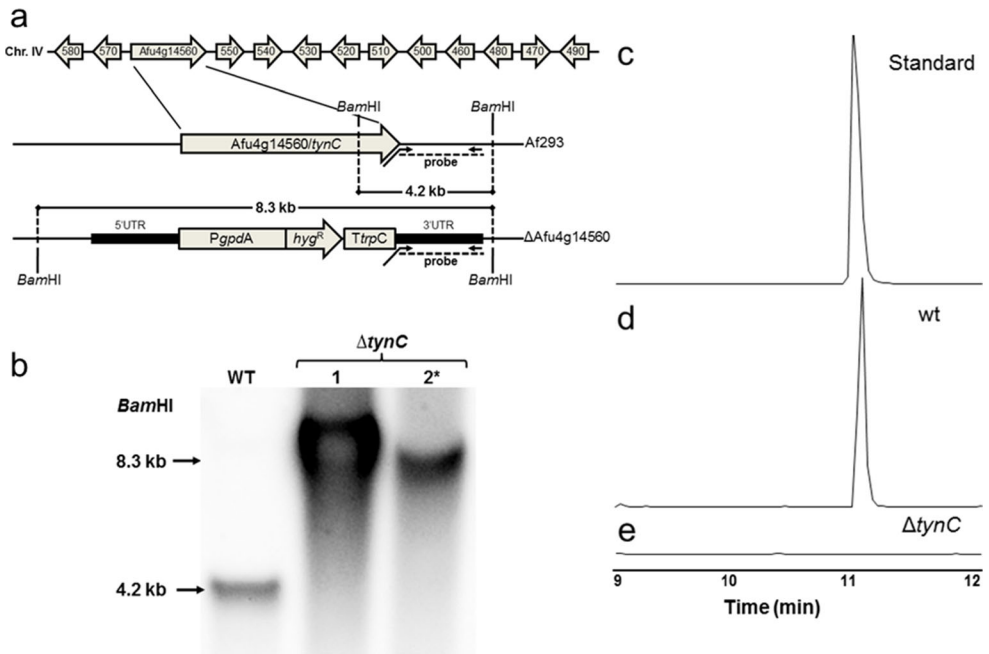

Fig. 2 PKS deletion mutant and chemical analysis. **a** Predicted putative trypacidin gene cluster (Gene ID: Afu4g14460-Afu4g14580) with the central gene being Afu4g14560/*tynC*, the PKS gene. *Lower panel* depicts the knock-out scheme for Afu4g14560/*tynC* by homologous recombination with the hygromycin resistance cassette. **b** Southern blot analysis of the knock-out mutants of Afu4g14560/*tynC*. Digestion with restriction enzyme *Bam*HI. WT (Af293), and of two deletion mutants: *1* and *2* (*asterisk* indicates deletion mutant used in all further tests). Restriction digest with *Bam*HI showed the signal of expected size for the wild-type of 4.2 kb and transformants of 8.3 kb indicative of the Afu4g14560/*tynC* deletion. **c** LC-MS profile of the extracted ion chromatogram (EIC) *m/z* 345 $[M + H]^+$ authentic trypacidin standard. **d** *A. fumigatus* wild-type Af293. **e** Δ*tynC* (Afu4g14560/*tynC* deletion knock-out)

Table 1 List of possible genes in the predicted trypacidin biosynthesis gene cluster and their putative function

Gene ID	Orthologe to *A. terreus*	% Amino acid identity	Putative function
Afu4g14460/*tynM*	ATEG_08456/*gedG*	61.0 %	Putative methyltransferase activity
Afu4g14470/*tynL*	ATEG_08457–1/*gedI*	60.0 %	Putative mdpH homolog
Afu4g14480/*tynK*	ATEG_08457–1/*gedH*	27.8 %	Putative emodin anthrone oxidase
Afu4g14490/*tynJ*	ATEG_08458/*gedJ*	62.6 %	Putative dihydrogeodin oxidase
Afu4g14500/*tynI*	ATET_08459/*gedK*	59.6 %	Putative Bayer Villiger-type oxidase
Afu4g14510/*tynH*	NA[a]	NA	Putative methyltransferase activity
Afu4g14520/*tynG*	ATEG_08455/*gedF*	76.4 %	Short-chain dehydrogenases/reductases
Afu4g14530/*tynF*	ATEG_08454/*gedE*	67.7 %	Theta class glutathione *S*-transferase
Afu4g14540/*tynE*	ATEG_08453/*gedR*	38.8 %	DNA binding, sequence-specific DNA binding transcription factor activity
Afu4g14550/*tynD*	ATEG_08452/*gedD*	42.1 %	Transcription coactivator activity
Afu4g14560/*tynC*	ATEG_08451/*gedC*	66.6 %	Non-reducing polyketide synthase
Afu4g14570/*tynB*	ATEG_08450/*gedB*	70.6 %	Has domain(s) with predicted hydrolase activity
Afu4g14580/*tynA*	ATEG_08449/*gedA*	72.7 %	Has domain(s) with predicted *O*-methyltransferase activity

[a] Indicates that this gene is not part of the geodin cluster in *A. terreus*

resolution mass spectrometry was applied comparing the wild-type strain to the *tynC* knock-out mutant (Fig. S4a, b in the Supplementary Material). In accordance with the proposed pathway, all intermediates were observed in the wild-type and not the mutant in all cases. Furthermore, the *tynC* knock-out mutant was fully complemented with the Afu4g14560/*tynC* PKS gene. This was confirmed by Southern blot and by LC-MS for the restoration of

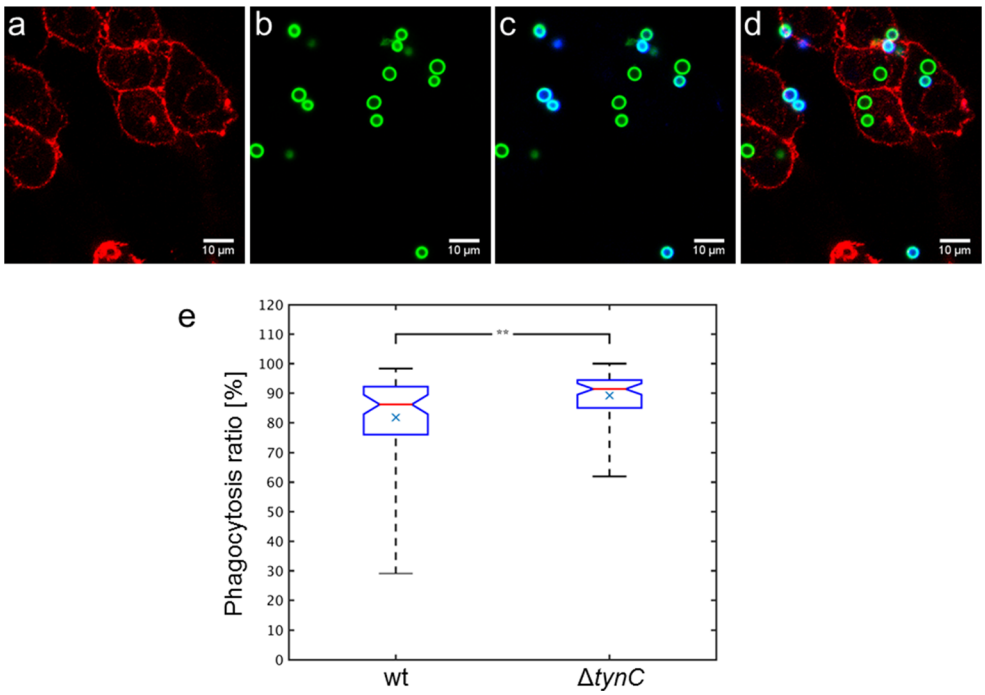

Fig. 3 Interaction of *A. fumigatus* Δ*tynC* conidia with macrophages. **a** Original image of macrophages stained with Alexa Fluor® 647 on the *red layer*. **b** *Green layer* with all FITC-labeled conidia. **c** *Green and blue layer* as overlay (FITC and calcofluor white) non-phagocytosed conidia in *blue*, phagocytosed conidia in *green*. **d** Overlay image of macrophages with phagocytosed and non-phagocytosed conidia. The *size bar* corresponds to 10 µm. **e** Determination of the phagocytosis ratio, i.e., the number of phagocytosed conidia over all macrophage-associated conidia. Co-incubation was determined after 1 h at 37 °C and 5 % CO_2 at an MOI of 7**.** *Centerlines* show the medians and notches represent their 95 % confidence interval; *box limits* indicate the 25th and 75th percentiles; *whiskers* exclude 2 % of the data points below and above as possible outliers; *crosses* represent the sample means for $n = 60$ sample points. *Asterisks* indicate significant p-values: *≥0.01 and <0.05; **≥0.001 and <0.01; ***<0.001; ns ≥0.05

trypacidin production in the mutant strain (Figs. S5a–e in the Supplementary Material).

Conidia of the *tynC* deletion mutant showed enhanced phagocytosis ratio by macrophages and amoebae

As trypacidin was found to represent a conidium-borne toxin of *A. fumigatus*, we tested whether trypacidin could play a role in the initial line of defense of the immune system. Interaction studies were conducted between *A. fumigatus* conidia, wild-type and *tynC* knock-out, with murine alveolar macrophages MH-S. Macrophages belong to the first lines of defense in mammals and are considered 'professional phagocytes.' Thus, the experiment entailed measuring the phagocytosis ratio. In order to obtain this measurement, 60 images per strain were analyzed by applying an algorithm for automated image analysis (Fig. 3a–d). This yielded 4907 conidia for the wild-type *Af*293 and 5026 conidia for the knock-out Δ*tynC*. The overall performance of the algorithm was evaluated by comparison with a manual analysis of 10 % of the image data (ground truth). The resulting performance measures yielded high values of 96.1 % for precision, 97.9 % for sensitivity, and 94.2 % for accuracy, which are comparable to performance measures reached in previous implementations (Mech et al. 2011, 2014; Kraibooj et al. 2014). The experiment showed that the mutant was phagocytosed significantly more often than the wild-type (Fig. 3e) with a mean value of 81.8 % for the wild-type and 89.2 % for the knock-out. Similarly, the median values are 86.2 and 91.4 % for the wild-type and knock-out, respectively.

A similar picture was obtained with the Dictyostelid amoeba, which were shown to be able to ingest conidia and are found in the same environment as *A. fumigatus* (Hillmann et al. 2015). As shown in Fig. 4a–d, *D. discoideum* phagocytosed both wild-type and Δ*tynC* conidia. However, counting of ingested conidia clearly indicated that the phagocytosis index (2 vs. 1.3 mean and 2 vs. 1 median values) for Δ*tynC* conidia was higher than for wild-type conidia (Fig. 4e). These data indicate that the conidium-bound trypacidin reduces phagocytosis of conidia by both the amoebae and macrophages.

Antiphagocytic activity of trypacidin

Since other studies demonstrated that trypacidin is a potent antiprotozoal against *T. cruzi* and *T. gondii*, we analyzed its bioactivity against *D. discoideum*. Pure trypacidin was toxic to *D. discoideum* and nearly complete growth inhibition was observed at concentrations above 30 μM. The IC_{50} value was determined to be 14 μM (Fig. S6 in the Supplementary Material), which is comparable to the values reported for *T. cruzi* and *T. gondii* or A549 lung epithelial cells (Ebringer et al. 1964, Gauthier et al. 2012). A minor, but significant effect on the viability of the amoeba was also visible when comparing conidia of *A. fumigatus* Af293 and the *tynC* deletion mutant. At an MOI of 2, the growth inhibition of the amoeba was more pronounced with wild-type conidia, 50 % viability compared to conidia devoid of trypacidin with over 70 % viable amoeba (Fig. 4f). Additionally, the CC_{50} value of trypacidin was assessed with alveolar macrophages MH-S (ATCC 2019) to determine how cytotoxic this spore-bound NP is to one of the first lines of defense of the mammalian immune system. The CC_{50} value was determined to be 0.65 μM (Fig. S7 in the Supplementary Material), which also showed to be cytotoxic compared to the amoeba and other protozoa tested.

Discussion

The antiprotozoal trypacidin has been a topic of research over the past 50 years, but since its discovery in the conidia of *A. fumigatus*, the genetic basis for its production has remained unknown (Nemec et al. 1963; Balan et al. 1963; Ebringer et al. 1963; Turner 1965). Identification of the responsible enzymes is, however, a prerequisite for the understanding of the biosynthesis pathway, its possible involvement in virulence, and potential biotechnological exploitations in the future. Finally, a gene can be deemed responsible for the main chemical scaffold. This compound has been known to have biological activity, in particular antiprotozoal, but, as shown here, it also has at least a significant effect on phagocytosis of conidia by macrophages and amoeboid phagocytes and thus might contribute to the infection process.

A. fumigatus, an infamous fungal pathogen, produces a variety of different compounds from the toxin, gliotoxin (Scharf et al. 2012, 2014b) to the indole-derived mycotoxins, ergot alkaloid-related clavines that are found throughout the fungal kingdom (Coyle and Panaccione 2005). Some of these compounds have been found to be involved in virulence of the fungus (Scharf et al. 2014a). Today, we know a few of the many notorious NPs produced by *A. fumigatus*, but there still remain many that can potentially be produced from the silent/cryptic biosynthesis gene clusters. Thus, in order to choose silent/cryptic gene clusters for further studies, one must assign the remaining orphan gene clusters to specific compounds to better select clusters that will give novel chemical scaffolds. One interesting compound whose biosynthesis has not been assigned to a gene cluster is trypacidin, which we have reported here.

The biological activity of trypacidin is of particular interest especially because of its localization to the conidia. This prompted the idea of trypacidin possibly playing a role in the phagocytosis of conidia. Phagocytosis is an active process, which requires the recognition of the pathogen-associated molecular patterns (PAMP) on the conidial surface. This is

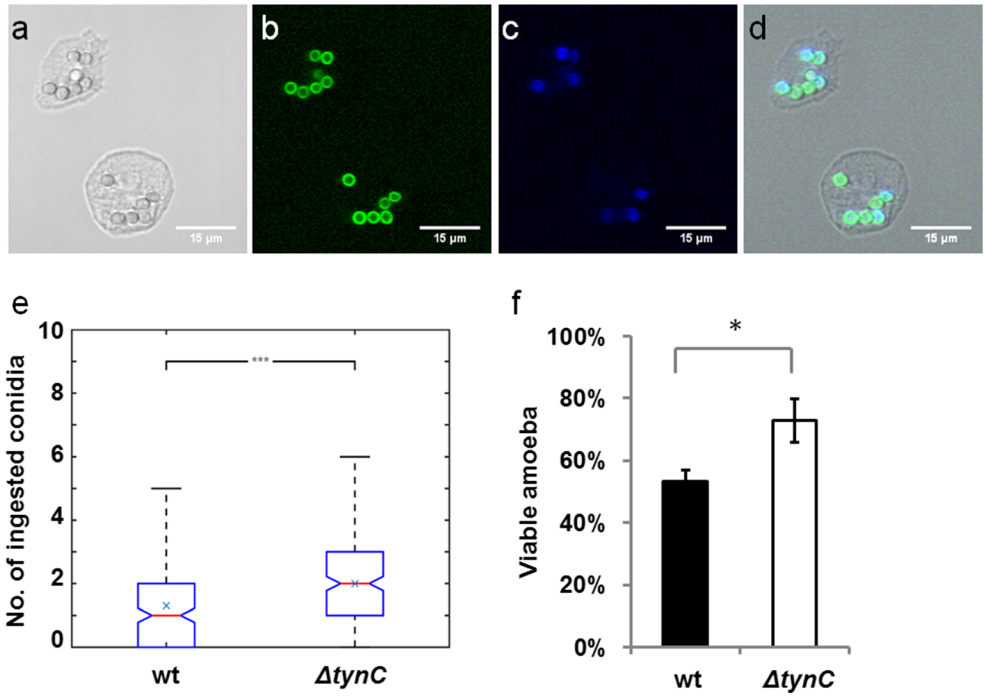

Fig. 4 Interaction of wild-type and *tynC*-mutant conidia with *D. discoideum*. **a**–**d** Phagocytosis of *A. fumigatus* conidia by *D. discoideum.* Conidia were FITC-stained (*green*) and incubated with *D. discoideum* at an MOI of 10. After 1 h, extracellular conidia (*blue*) were counter-stained with CFW and analyzed by fluorescence microscopy. Phagocytic interactions are shown as a brightfield image (**a**), images of the *green* (**b**) and *blue* channel (**c**), as well as an overlay of all three images (**d**). **e** Phagocytic index of conidia. Images were used to determine the number of ingested conidia (*green*) per amoeba cell. *Centerlines* show the medians and notches represent their 95 % confidence interval; *box limits* indicate the 25th and 75th percentiles; *whiskers* exclude 2 % of the data points below and above as possible outliers; *crosses* represent the sample means for $n = 200$ sample points. *Asterisks* indicate significant values: *≥0.01 and <0.05; **≥0.001 and <0.01; ***<0.001; ns ≥0.05. **f** Wild-type (*filled column*) and *tynC* deletion mutant conidia (*open column*) of *A. fumigatus* were co-incubated with *D. discoideum* at an MOI of 2. After 24 h at 22 °C, viable amoebae cells were counted using CASY® TT Cell Counter, and values are expressed as the percentage of cells vs. conidia free controls. An *asterisk* indicates statistical significance in a Student's *t* test with a *p* value <0.05

achieved by pattern recognition receptors (PRRs) like dectin-1, TLR-2, and TLR-4 on the cell surface of immune cells (Meier et al. 2003; Netea et al. 2003; Steele et al. 2005; Chai et al. 2011). Dectin-1 binds β-(1, 3)-glucan and thus recognizes fungal pathogens (Luther et al. 2007). The level of recognition of the pathogen by macrophages is measured with the phagocytosis assay. Interestingly, a significant difference in phagocytosis ratio between the wild-type Af293 strain and the *tynC* knock-out mutant was observed. Furthermore, it could be shown that trypacidin interfered with the active process of phagocytosis since the knock-out mutant was phagocytosed more than the wild-type by both amoeboid phagocytes and macrophages. This could imply that trypacidin reduces the recognition/uptake of the conidia by the macrophage or slows down phagocytosis. A similar result was also observed for the DHN-melanin-deficient mutant, *pksP*, where macrophages also recognized and phagocytosed the mutant conidia more frequently (Thywißen et al. 2011; Mech et al. 2011; Luther et al. 2007). Additionally, this mutant was also shown to be less virulent in the mouse infection model (Jahn et al. 1997). Furthermore, this particular mutant was phagocytosed more efficiently by the amoeba *D. discoideum* (Hillmann et al. 2015), thus showing the importance of DHN-melanin in interfering with the recognition of fungal conidia. Moreover, Van Waeyenberghe et al. (2013) demonstrated that the amoeba *A. castellanii* was also able to phagocytose *A. fumigatus* conidia. But in both cases, *A. fumigatus* was able to successfully germinate inside of the amoeba in vitro and essentially killed the amoebae. This observation was also confirmed in vitro with macrophages where the phagocytosed fungus can avoid being harmed and after a while can kill the macrophage by germination (Kurup 1984). These two examples indicate how coevolution could take place. Phagocytic cells cause the fungus to develop counterstrategies and protect its spores. Since conidia are the metabolically inactive form of *A. fumigatus*, the fungus is incapable of defending itself actively. To overcome this fact, the fungus arms its conidia with a wide variety of NPs. To prevent recognition by phagocytic cells, conidia possess a proteinaceous layer consisting of RodA that is immunologically inert (Aimanianda et al. 2009). In case of the uptake by phagocytic cells, the DHN-melanin layer of conidia is able to inhibit the acidification of the phagolysosome (Thywißen et al. 2011). Consequently, conidia escape killing and can germinate from the phagolysosome. Here, we have shown that trypacidin is

another protective NP bound to the conidium of *A. fumigatus* that appears to inhibit phagocytic cells to further enhance survival.

Acknowledgments We thank Carmen Schult and Eva-Maria Neumann for excellent technical assistance, Andrea Perner for HRMS measurements, and Franziska Schmidt for macrophage cultivations. We also thank Thorsten Heinekamp and Maria Straßburger for insightful conversations. This work was supported by the Deutsche Forschungsgemeinschaft (DFG)-funded Graduate School of Excellence, Jena School for Microbial Communication, and the DFG-funded collaborative research center / Transregio (SFB/TR) 124 Human-pathogenic fungi and their human host–networks of interaction FungiNet (project A1 to AB and project B4 to MTF).

Conflict of interest The authors declare that they have no conflict of interest.

References

Aimanianda V, Bayry J, Bozza S, Kniemeyer O, Perruccio K, Elluru SR, Clavaud C, Paris S, Brakhage AA, Kaveri SV, Romani L, Latgé JP (2009) Surface hydrophobin prevents immune recognition of airborne fungal spores. Nature 460(7259):1117–1121

Balan J, Ebringer L, Nemec P (1964) Trypacidin a new antiprotozoal antibiotic. Naturwissenschaften 51(9):227

Balan J, Ebringer L, Nemec P, Kovac S, Dobias J (1963) Antiprotozoal antibiotics. II. Isolation and characterization of trypacidin, a new antibiotic, active against *Trypanosoma cruzi* and *Toxoplasma gondii*. J Antibiot (Tokyo) 6:157–160

Baldin C, Valiante V, Krüger T, Schafferer L, Haas H, Kniemeyer O, Brakhage AA (2015) Comparative proteomics of a tor inducible *Aspergillus fumigatus* mutant reveals involvement of the *Tor* kinase in iron regulation. Proteomics 15(13):2230–2243

Brakhage AA (2013) Regulation of fungal secondary metabolism. Nat Rev Microbiol 11(1):21–32

Brakhage AA, Langfelder K (2002) Menacing mold: the molecular biology of *Aspergillus fumigatus*. Annu Rev Microbiol 56:433–455

Brakhage AA (2005) Systemic fungal infections caused by *Aspergillus* species: epidemiology, infection process and virulence determinants. Curr Drug Targets 6(8):875–886

Bergmann S, Schümann J, Scherlach K, Lange C, Brakhage AA, Hertweck C (2007) Genomics-driven discovery of PKS-NRPS hybrid metabolites from *Aspergillus nidulans*. Nat Chem Biol 3(4): 213–217

Berthier E, Lim FY, Deng Q, Guo CJ, Kontoyiannis DP, Wang CC, Rindy J, Beebe DJ, Huttenlocher A, Keller NP (2013) Low-volume toolbox for the discovery of immunosuppressive fungal secondary metabolites. PLoS Pathog 9(4): e1003289

Cerqueira GC, Arnaud MB, Inglis DO, Skrzypek MS, Binkley G, Simison M, Miyasato SR, Binkley J, Orvis J, Shah P, Wymore F, Sherlock G, Wortman JR (2013) The *Aspergillus* genome database (AspGD): multispecies curation and incorporation of RNA-Seq data to improve structural gene annotations. Nucl Acids Res 42(Database issue):D705–D710

Chai LY, Vonk AG, Kullberg BJ, Verweij PE, Verschueren I, van der Meer JW, Joosten LA, Latgé JP, Netea MG (2011) *Aspergillus fumigatus* cell wall components differentially modulate host TLR2 and TLR4 responses. Microbes Infect 13(2):151–159

Chiang YM, Szewczyk E, Davidson AD, Entwistle R, Keller NP, Wang CC, Oakley BR (2010) Characterization of the *Aspergillus nidulans* monodictyphenone gene cluster. Appl Environ Microbiol 76(7): 2067–2074

Chooi YH, Fang J, Liu H, Filler SG, Wang P, Tang Y (2013) Genome mining of a prenylated and immunosuppressive polyketide from pathogenic fungi. Org Lett 15(4):780–783

Coyle CM, Panaccione DG (2005) An ergot alkaloid biosynthesis gene and clustered hypothetical genes from *Aspergillus fumigatus*. Appl Environ Microbiol 71(6):3112–3118

Ebringer L, Catar G, Balan J, Nemec P, Kov'ac S (1963) Antiprotozoal antibiotics. III Preliminary Report on the Effect of Trypacidin on Experimental Toxoplasmosis J Antibiot (Tokyo) 16:161–162

Ebringer L, Balan J, Nemec P (1964) Incidence of antiprotozoal substances in *Aspergillaceae*. J Protozool 11(2):153–156

Fischer G, Müller T, Ostrowski R, Dott W (1999) Mycotoxins of *Aspergillus fumigatus* in pure culture and in native bioaerosols from compost facilities. Chemosphere 38(8):1745–1755

Frisvad JC, Rank C, Nielsen KF, Larsen TO (2009) Metabolomics of *Aspergillus fumigatus*. Med Mycol 47(Suppl 1):S72–S79

Gauthier T, Wang X, Sifuentes Dos Santos J, Fysikopoulos A, Tadrist S, Canlet C, Artigot MP, Loiseau N, Oswald IP, Puel O (2012) Trypacidin, a spore-borne toxin from *Aspergillus fumigatus*, is cytotoxic to lung cells. PLoS One 7(2):e29906

Gibson DG, Young L, Chuang RY, Venter JC, Hutchison III CA, Smith HO (2009) Enzymatic assembly of DNA molecules up to several hundred kilobases. Nat Methods 6(5):343–345

Guo CJ, Wang CC (2014) Recent advances in genome mining of secondary metabolites in *Aspergillus terreus*. Front Microbiol 23(717):1–13

Heinekamp T, Schmidt H, Lapp K, Pähtz V, Shopova I, Köster-Eiserfunke N, Krüger T, Kniemeyer O, Brakhage AA (2015) Interference of *Aspergillus fumigatus* with the immune response. Semin Immunpathol 37(2):141–152

Hillmann F, Novohradská S, Mattern DJ, Forberger T, Heinekamp T, Westermann M, Winckler T, Brakhage AA (2015) Virulence determinants of the human pathogenic fungus *Aspergillusfumigatus* protect against soil amoeba predation. Environ Microbiol doi:. doi:10.1111/1462-2920.12808

Ibrahim-Granet O, Philippe B, Boleti H, Boisvieux-Ulrich E, Grenet D, Stern M, Latgé JP (2003) Phagocytosis and intracellular fate of *Aspergillus fumigatus* conidia in alveolar macrophages. Infect Immun 71(2):891–903

Jahn B, Koch A, Schmidt A, Wanner G, Gehringer H, Bhakdi S, Brakhage AA (1997) Isolation and characterization of a pigmentless-conidium mutant of *Aspergillus fumigatus* with altered conidial surface and reduced virulence. Infect Immun 65(12):5110–5117

Kraibooj K, Park HR, Dahse HM, Skerka C, Voigt K, Figge MT (2014) Virulent strain of *Lichtheimia corymbifera* shows increased phagocytosis by macrophages as revealed by automated microscopy image analysis. Mycoses Suppl 3:56–66

König CC, Scherlach K, Schroeckh V, Horn F, Nietzsche S, Brakhage AA, Hertweck C (2013) Bacterium induces cryptic meroterpenoid pathway in the pathogenic fungus *Aspergillus fumigatus*. Chembiochem 14(8):938–942

Kurup VP (1984) Interaction of *Aspergillus fumigatus* spores and pulmonary alveolar macrophages of rabbits. Immunobiology 166(1):53–61

Lim FY, Hou Y, Chen Y, Oh JH, Lee I, Bugni TS, Keller NP (2012) Genome based cluster deletion reveals an endocrocin biosynthetic pathway in *Aspergillus fumigatus*. Appl Environ Microbiol 78(12): 4117–4125

Luther K, Torosantucci A, Brakhage AA, Heesemann J, Ebel F (2007) Phagocytosis of *Aspergillus fumigatus* conidia by murine macrophages involves recognition by the dectin-1 β-glucan receptor and toll-like receptor 2. Cell Microbiol 9(2):368–381

Maerker C, Rohde M, Brakhage AA, Brock M (2005) Methylcitrate synthase from *Aspergillus fumigatus*. Propionyl-CoA affects

polyketide synthesis, growth and morphology of conidia. FEBS J 272(14):3615–3630

Marchler-Bauer A, Panchenko AR, Shoemaker BA, Thiessen PA, Geer LY, Bryant SH (2002) CDD: a database of conserved domain alignments with links to domain three-dimensional structure. Nucl Acids Res 30(1):281–283

Mech F, Thywissen A, Guthke R, Brakhage AA, Figge MT (2011) Automated image analysis of the host-pathogen interaction between phagocytes and *Aspergillus fumigatus*. PLoS One 6(5):e19591

Mech F, Wilson D, Lehnert T, Hube B, Figge MT (2014) Epithelial invasion outcompetes hypha development during *Candida albicans* infection as revealed by an image-based systems biology approach. Cytometry A 85(2):126–139

Meier A, Kirschning CJ, Nikolaus T, Wagner H, Heesemann J, Ebel F (2003) Toll-like receptor (TLR) 2 and TLR4 are essential for *Aspergillus*-induced activation of murine macrophages. Cell Microbiol 5(8):561–570

Nemec P, Balan J, Ebringer L (1963) Antiprotozoal antibiotics. I J Antibiot (Tokyo) 16:155–156

Netea MG, Warris A, Van der Meer JW, Fenton MJ, Verver-Janssen TJ, Jacobs LE, Andresen T, Verweij PE, Kullberg BJ (2003) *Aspergillus fumigatus* evades immune recognition during germination through loss of toll-like receptor-4-mediated signal transduction. J Infect Dis 188(2):320–326

Nielsen ML, Nielsen JB, Rank C, Klejnstrup ML, Holm DK, Brogaard KH, Hansen BG, Frisvad JC, Larsen TO, Mortensen UH (2011) A genome-wide polyketide synthase deletion library uncovers novel genetic links to polyketides and meroterpenoids in *Aspergillus nidulans*. F E M S Microbiol Lett 321(2):157–166

Nielsen MT, Nielsen JB, Anyaogu DC, Holm DK, Nielsen KF, Larsen TO, Mortensen UH (2013) Heterologous reconstitution of the intact geodin gene cluster in *Aspergillus nidulans* through a simple and versatile PCR based approach. PLoS One 8(8):e72871

Parker GF, Jenner PC (1968) Distribution of trypacidin in cultures of *Aspergillus fumigatus*. Appl Microbiol 16(8):1251–1252

Philippe B, Ibrahim-Granet O, Prévost MC, Gougerot-Pocidalo MA, Sanchez Perez M, Van der Meeren A, Latgé JP (2003) Killing of *Aspergillus fumigatus* by alveolar macrophages is mediated by reactive oxidant intermediates. Infect Immun 71(6):3034–3042

Scharf DH, Heinekamp T, Remme N, Hortschansky P, Brakhage AA, Hertweck C (2012) Biosynthesis and function of gliotoxin in *Aspergillus fumigatus*. Appl Microbiol Biotechnol 93(2):467–472

Scharf DH, Heinekamp T, Brakhage AA (2014a) Human and plant fungal pathogens: the role of secondary metabolites. PLoS Pathog 10(1): e1003859

Scharf DH, Habel A, Heinekamp T, Brakhage AA, Hertweck C (2014b) Opposed effects of enzymatic gliotoxin N- and S-methylations. J Am Chem Soc 136(33):11674–11679

Steele C, Rapaka RR, Metz A, Pop SM, Williams DL, Gordon S, Kolls JK, Brown GD (2005) The β-glucan receptor dectin-1 recognizes specific morphologies of *Aspergillus fumigatus*. PLoS Pathog 1(4): e42

Szewczyk E, Nayak T, Oakley CE, Edgerton H, Xiong Y, Taheri-Talesh N, Osmani SA, Oakley BR (2006) Fusion PCR and gene targeting in *Aspergillus nidulans*. Nat Protoc 1(6):3111–3120

Szewczyk E, Chiang YM, Oakley CE, Davidson AD, Wang CCC, Oakley BR (2008) Identification and characterization of the asperthecin gene cluster of *Aspergillus nidulans*. Appl Environ Microbiol 74(24):7607–7612

Tae H, Sohng JK, Park K (2009) MapsiDB: an integrated web database for type I polyketide synthases. Bioprocess Biosyst Eng 32(6):723–727

Then Bergh KT, Litzka O, Brakhage AA (1996) Identification of a major *cis*-acting DNA element controlling the bidirectionally transcribed penicillin biosynthesis genes *acvA* (*pcbAB*) and *ipnA* (*pcbC*) of *Aspergillus nidulans*. J Bacteriol 178(13):3908–3916

Thywißen A, Heinekamp T, Dahse HM, Schmaler-Ripcke J, Nietzsche S, Zipfel PF, Brakhage AA (2011) Conidial dihydroxynaphthalene melanin of the human pathogenic fungus *Aspergillus fumigatus* interferes with the host endocytosis pathway. Front Microbiol 2:96

Turner WB (1965) The production of trypacidin and monomethylsulochrin by *Aspergillus fumigatus*. J Chem Soc 6658-6659

Unkles SE, Valiante V, Mattern DJ, Brakhage AA (2014) Synthetic biology tools for bioprospecting of natural products in eukaryotes. Chem Biol 21(4):502–508

Van Waeyenberghe L, Baré J, Pasmans F, Claeys M, Bert W, Haesebrouck F, Houf K, Martel A (2013) Interaction of *Aspergillus fumigatus* conidia with *Acanthamoeba castellanii* parallels macrophage-fungus interactions. Environ Microbiol Rep 5(6): 819–824

Yaegashi J, Oakley BR, Wang CC (2014) Recent advances in genome mining of secondary metabolite biosynthetic gene clusters and the development of heterologous expression systems in *Aspergillus nidulans*. J Ind Microbiol Biotechnol 41(2):433–442